Facial Plastic Surgery & Aesthetic Medicine
Volume 00, Number 00, 2025

DOI: 10.1177/26893614251395737

Facial Plastic Surgery & Aesthetic Medicine

A video of this technique is available online.

ORIGINAL INVESTIGATION **Facial Nerve**

Use of Dynamic, Automated Facial Analysis in Quantifying Oral-Ocular Synkinesis

Angela Renne, BS,[1] Jeffrey Heaton, PhD,[2] Adeeb Derakhshan, MD,[3] Jason C. Nellis, MD,[1] Shaun C. Desai, MD,[1] and Kofi D.O. Boahene, MD[1,*]

Abstract

Background: Oral-ocular synkinesis is a frequent sequela of idiopathic facial paralysis (IFP), yet objective, dynamic methods to quantify associated palpebral fissure changes remain limited.

Objective: To objectively measure palpebral changes in IFP using automated facial tracking.

Design Type: Case-control.

Methods: A novel, video-based facial tracking software assessed facial expressions in 12 controls and 30 IFP cases with synkinesis at least 12 months from onset of IFP. Palpebral fissure dimensions were measured at rest and during smile, laugh, and pucker. Bilateral differences across expressions were analyzed using Wilcoxon signed-rank, Kruskal-Wallis, and linear regression.

Results: Puckering showed the greatest asymmetry ($p < 0.001$), with a 30.0% reduction in palpebral fissure size on the paralyzed side versus 21.6% on the non-paralyzed side, compared to a 1.7% reduction in controls. No significant differences were observed between paralyzed and non-paralyzed sides during rest-to-smile or rest-to-laugh expressions. Dynamic modeling found that puckering elicited the fastest and largest decline in palpebral fissure symmetry (slope = –0.196; standard error: 0.011; $p < 0.001$). Paralysis duration following 12 months had no significant effect on palpebral fissure changes.

Conclusion: Dynamic facial tracking effectively quantifies expression-specific disruptions in oral-ocular coordination in IFP, particularly during puckering, offering objective data to support treatment planning and patient counseling.

Introduction

Idiopathic facial paralysis (IFP) is an acute, unilateral facial nerve disorder affecting ∼1 in 60–70 individuals over a lifetime.[1] While most patients recover, up to 30% develop persistent complications, most notably oral-ocular synkinesis, a phenomenon in which voluntary oral movements trigger involuntary eye closure.[2–5] Although commonly recognized, the dynamics of synkinesis remain poorly quantified.[6] The pathophysiology of synkinesis is thought to involve aberrant facial nerve regeneration, leading to the involuntary coupling of facial movements.[7–9] However, alternative explanations for synkinesis, such as facial nuclear hyperexcitability have been proposed due to the predictability and timing of synkinetic patterns.[4,10–12] Synkinesis imposes significant functional and psychosocial burdens, often due to its conspicuous and involuntary nature.[7,13]

Palpebral fissure measurements have long served as an objective metric in facial paralysis research, providing insight into both functional and aesthetic outcomes.[6,14,15] However, prior studies largely relied on static photography

[1]*Division of Facial Plastic and Reconstructive Surgery, Department of Otolaryngology—Head and Neck Surgery, Johns Hopkins School of Medicine, Baltimore, Maryland, USA.*
[2]*McKelvey School of Engineering, Washington University in St. Louis, St. Louis, Missouri, USA.*
[3]*Department of Otolaryngology—Head and Neck Surgery, Loma Linda University, Loma Linda, California, USA.*

*Address correspondence to: *Kofi D.O. Boahene, MD, 601 N Caroline Street, 6th floor, Baltimore MD 21287, USA*, Email: dboahen1@jhmi.edu

KEY POINTS

Question: Can facial tracking technology (DynaFace) help analyze and quantify synkinetic eyelid movement in people with idiopathic facial paralysis (IFP)?

Findings: DynaFace reliably quantified and analyzed the temporal pattern of palpebral fissure changes (corneal surface coverage) in oral-ocular synkinesis. Individuals with IFP show greater involuntary eye narrowing during puckering, which can be objectively assessed using dynamic facial analysis.

Meaning: This approach may offer a more consistent way to evaluate facial nerve recovery and personalized treatment strategies for patients with IFP.

or subjective grading systems (e.g., House–Brackmann, Sunnybrook), which fail to capture dynamic, expression-dependent eyelid behavior.[16–24] While these approaches are useful for overall assessment, they lack quantitative and temporal details of how oral movement uniquely impacts palpebral fissure dynamics in oral-ocular synkinesis.

Recent advances in computer vision and artificial intelligence (AI) enable reliable, real-time tracking of subtle facial dynamics. To address the limitations of traditional assessments, we developed DynaFace, an open-access, video-based facial tracking platform. DynaFace integrates deep convolutional neural networks with adaptive temporal modeling to capture micro-expressions, rapid movements, and complex spatial-temporal patterns with high fidelity. Its modular design supports analysis at both the subunit and whole-face levels, providing automated, objective measurements such as synkinetic palpebral fissure dynamics.[25] By combining convolutional networks for fine-grained landmark detection with graph attention regressors that model spatial relationships, DynaFace captures both local detail and global structure.[26,27] Unlike conventional methods that assume symmetry,[28] DynaFace uses attention mechanisms to identify stable landmarks across the entire face, enabling accurate tracking even in asymmetrical conditions like facial paralysis. In doing so, it delivers precise, quantitative assessments of facial movement that surpass traditional visual grading.

In this study, we apply DynaFace to a clinically challenging context: quantifying eyelid motion and oral-ocular synkinesis in longstanding IFP. This setting, characterized by subtle, asymmetrical, and temporally variable movements, tests the system's ability to resolve fine-grained trajectories under irregular conditions. Our goal was to characterize expression-dependent changes in palpebral fissure and assess dynamics between the paralyzed and non-paralyzed sides. We hypothesized that DynaFace would detect significant asymmetries, supporting its role as an objective, reproducible tool for evaluating synkinesis and informing treatment strategies in facial paralysis.

Methods

Participant population

We conducted a case-control study of 30 patients with IFP and synkinesis and 12 healthy controls to assess bilateral palpebral fissure changes during oral movements. Inclusion required ≥12 months since IFP onset and clinical evidence of synkinesis. Patients with other facial nerve disorders or prior surgical interventions such as myectomy or neurectomy/neurolysis were excluded. Those with a history of botulinum toxin treatment were eligible only if ≥3 months had elapsed since their last injection. The 12 healthy controls were included to provide baseline palpebral fissure changes for comparison with paralyzed and non-paralyzed hemifaces.

DynaFace

This study represents the first clinical application of DynaFace for objective facial movement analysis, using a challenging test case to demonstrate its capabilities and detail the underlying methodology. DynaFace is an open-access, AI-driven facial landmark tracking system that employs deep machine learning to enable reproducible, quantitative assessment of facial dynamics. It identifies 95 standardized landmarks across both hemifaces (Fig. 1), forming the basis for calculating clinically relevant movement metrics.

DynaFace integrates two neural network models. The first, SPIGA (Shape Preserving Inference of Graph Attention networks), is a cascade graph attention network that preserves local and global facial geometry while correcting for head pose variation (pitch, roll, and yaw) by projecting three-dimensional coordinates onto a two-dimensional image space.[27] The second, FaceNet, is a deep convolutional embedding network that provides robust facial alignment, previously validated on large-scale facial recognition databases for accuracy and stability.[26] Together, these networks extract fine-grained landmarks, irrespective of pose, that remain reliable in asymmetrical or pathological faces.

From these landmarks, DynaFace quantifies several clinically relevant features, including bilateral oral commissure excursion, palpebral fissure area, brow elevation, dental show area, and the Facial Asymmetry Index (FAI), defined as the linear distance between the oral commissure and medial canthus on each side. Surface area estimates are derived from two-dimensional projections using the shoelace algorithm, with pixel distances scaled to millimeters based on a standardized interpupillary distance of 63 mm. Pixel-based area calculations were cross-validated against Adobe Photoshop measurements to ensure geometric accuracy. To confirm robustness in clinical settings, landmark placement was manually reviewed in 30 symmetric and 30 asymmetrical faces, validating both precision and reliability in cases of facial paralysis

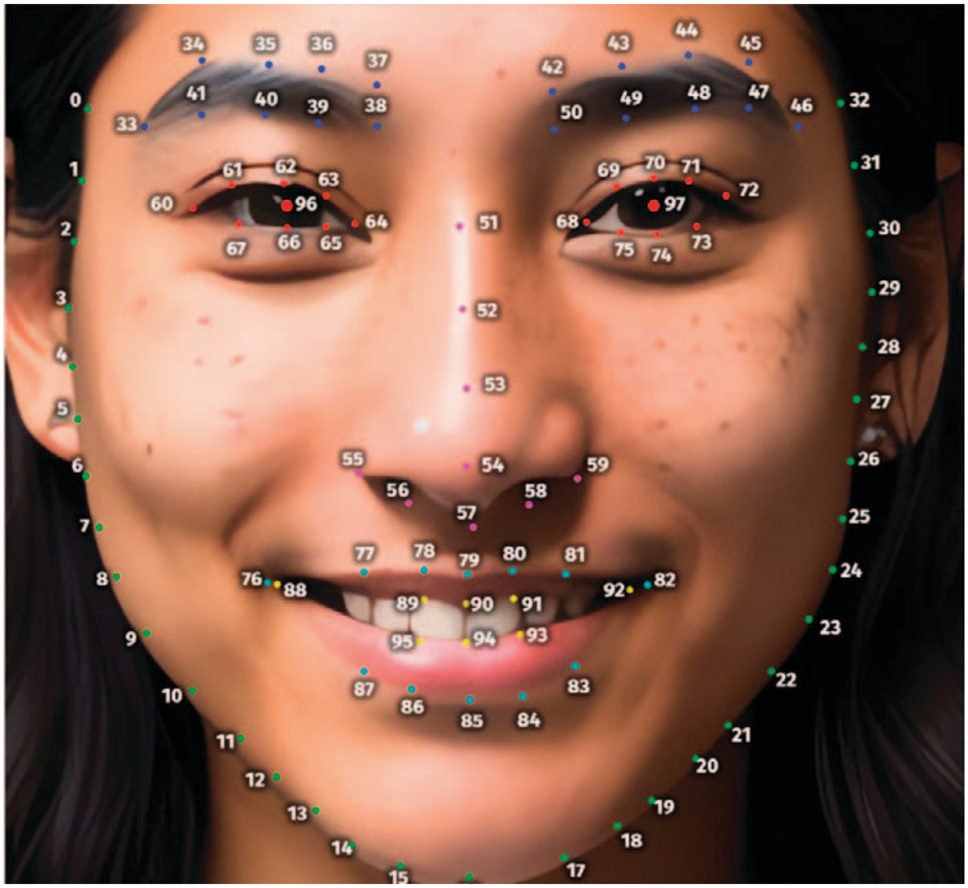

Fig. 1. DynaFace Landmarks. DynaFace is a facial landmark tracking system that uses 95 standardized points to capture facial movement across both hemifaces. Landmarks span key regions including the brows, eyes, nose, cheeks, mouth, and jaw. Movements are measured by tracking changes from rest, allowing objective analysis of facial expression and symmetry.

and other etiologies of facial asymmetry. As such, DynaFace offers a reproducible, scalable platform for objective facial movement analysis and capturing clinically relevant changes in facial function.

Study procedures

After obtaining consent, participants underwent standardized video recording of facial expressions. Using DynaFace, a novel facial tracking software (pre-release version available at https://github.com/jeffheaton/dynaface), we recorded dynamic facial movements transitioning from rest to three volitional expressions: smile, laugh, and pucker. Participants were given standardized verbal instructions with brief pauses between commands to complete each movement. To reduce ambiguity and variability, expressions were explicitly defined: for the smile, participants were instructed, “Please smile like you’re posing for a picture”; for the laugh, “Give a big laugh as if you’re laughing at a joke.” As the goal of the project is to study oral-ocular synkinesis, we used these cues to emphasize intentional oral movements to best capture resulting palpebral fissure dynamics.

As such, this study focused specifically on changes in palpebral fissure dimensions during elicited oral movements in patients with synkinesis. We used DynaFace to quantify these palpebral changes through automated tracking of ocular landmarks (see Supplementary Video for example and plotting of palpebral fissure ratio). Measurements were recorded in square millimeters (mm^2), with percent changes calculated from resting baseline values. For IFP patients, both paralyzed and non-paralyzed sides were analyzed to assess asymmetry. This study was reviewed and approved by the Johns Hopkins Medicine Institutional Review Board (IRB00422662).

Outcomes of interest

Palpebral fissure changes were evaluated using both static and dynamic analyses. For static analysis, DynaFace quantified fissure area at rest and at peak expression for smile, laugh, and pucker. Percent changes from rest to maximal expression were calculated, and median values with interquartile ranges (IQRs) were compared between paralyzed and non-paralyzed hemifaces. In controls, right and left sides were similarly assessed.

Dynamic analysis involved frame-by-frame tracking of palpebral fissure dimensions across the full expression sequence (approximately 30 frames per second). Temporal plots were generated to visualize changes over time. In patients, the ratio of paralyzed to non-paralyzed palpebral fissure was computed across frames to evaluate evolving asymmetry. In controls, right-to-left eye ratios assessed normal bilateral coordination. The frame immediately preceding facial movement was defined as $t = 0$, establishing the resting baseline for subsequent comparisons.

Statistical analysis

Summary statistics and Wilcoxon signed-rank tests were used in cases to compare the dimensions of the paralyzed and non-paralyzed palpebral fissures at rest and during smile, laugh, and pucker. Kruskal-Wallis tests were employed to evaluate the differences across facial expressions of palpebral fissure measurements from rest to peak expression in controls and in paralyzed and non-paralyzed hemifaces in cases. Univariate linear regression assessed whether the duration of facial paralysis influenced hemifacial changes in palpebral fissure areas from rest. To assess dynamic asymmetry, linear regression was used to calculate the slope, SE, and significance of the palpebral fissure ratio (paralyzed/non-paralyzed) over time for each expression. Statistical significance was set at $p < 0.05$. All analyses were conducted in R (version 4.4.0, R Core Team, 2024).

Results

Study population

The IFP group ($n = 30$) had a median age of 51 years (IQR: 47–58). For sex, 23.1% were male, and 76.9% were female. All IFP patients had completed their acute recovery period and demonstrated evidence of synkinesis. The median duration of paralysis was 24.5 months (IQR: 16.6–34.8).

Palpebral fissure assessment

Palpebral fissure areas were assessed using DynaFace at rest and during smile, laugh, and pucker expressions. At rest, both sides were similar: non-paralyzed (median 190 mm^2, IQR: 179–230) and paralyzed (190 mm^2, IQR: 172–211). During smile, the non-paralyzed side measured 149 mm^2 (IQR: 113–184) versus 134 mm^2 (IQR: 112–164) on the paralyzed side. For laugh, values were 128 mm^2 (IQR: 88.8–155) and 102 mm^2 (IQR: 73.4–141), respectively. Pucker showed the greatest difference: non-paralyzed 171 mm^2 (IQR: 142–208) versus paralyzed 132 mm^2 (IQR: 115–157).

Comparison of IFP hemifaces

Statistical analysis using Wilcoxon signed-rank revealed no significant difference in palpebral fissure area between the paralyzed and non-paralyzed sides during positions at rest (median difference: 0.21 mm^2; $p = 0.085$). However, significant asymmetries were observed at peak expression during smiling (14.96 mm^2; $p = 0.018$), laughing (25.54 mm^2; $p = 0.0077$) and puckering (39.16 mm^2; $p = 0.0028$), with the paralyzed side reduced compared to the non-paralyzed hemiface (Fig. 2).

Dimensions compared to resting baseline

Analysis of palpebral fissure changes from rest to peak expression during smile, laugh, and pucker revealed the greatest asymmetry during puckering (Fig. 3). The paralyzed side had a median reduction of 30.0% (IQR: −37.5%, −21.6%), significantly greater than the non-paralyzed side (21.6%, IQR: −27.7%, −3.3%) and controls (1.7%, IQR: −12.6%, 4.7%; $p < 0.001$). During smiling, reductions were found across all groups: median 27.1% (paralyzed, IQR: −43.4% to −16.9%), 22.5% (non-paralyzed, IQR: −33.4% to −16.7%), and 23.2% (controls, IQR: −26.3% to −9.2%; $p = 0.09$). Laughing elicited large reductions across all groups: 43.3% (paralyzed, IQR: −58.3% to −34.5%), 37.2% (non-paralyzed, IQR: −47.5% to −26.3%), and 38.6% (controls, IQR: −56.4% to −22.5%), without significant group differences ($p = 0.22$).

Assessing paralysis duration

Duration was not significantly associated with percent change in palpebral fissure area for any expression or side (Table 1). For the paralyzed hemiface, estimated effects of duration ranged from −0.014 ± (SE) 0.032 (smile; $p = 0.66$) to 0.032 ± 0.034 (laugh; $p = 0.36$). Similarly, for the non-paralyzed side, coefficients ranged from −0.040 ± 0.033 (smile; $p = 0.24$) to 0.007 ± 0.033 (pucker; $p = 0.84$).

Temporal expression dynamics of palpebral fissure ratios in IFP and controls

Temporal analysis of palpebral fissure ratios of the right and left eyes reveals that in the control group, ratios remained around 1.0 across all expressions, exhibiting minimal variation and asymmetry over time (Fig. 4). In contrast, the IFP group demonstrated distinct temporal patterns in the paralyzed/non-paralyzed palpebral fissure ratio.

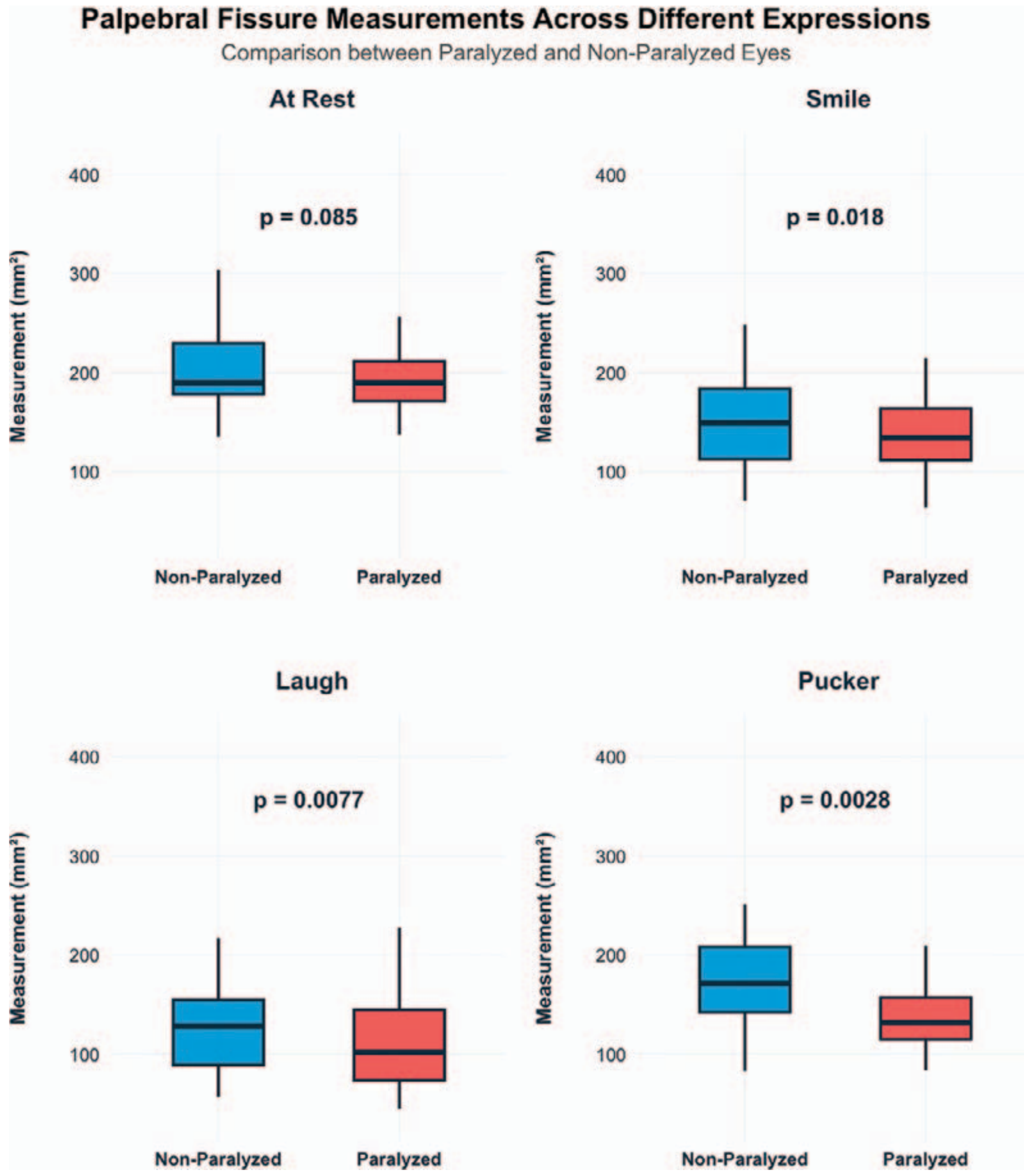

Fig. 2. Median and Distribution of Palpebral Fissures Across Facial Expressions. Medians (in mm^2) between paralyzed and non-paralyzed sides in idiopathic facial paralysis (IFP) patients during rest, smile, laugh, and pucker expressions. Boxplots represent value distribution. Statistically significant asymmetry was observed during smile, laugh and pucker expressions ($p = 0.018$, 0.0077, and $p = 0.0028$, respectively), while differences during rest were not significant. Data derived from Wilcoxon signed-rank tests.

For the laugh expression, which had the greatest overall reduction in palpebral fissure dimensions (43.3% in the paralyzed eye, 37.2% in the non-paralyzed eye, 38.6% in controls), linear modeling revealed a statistically significant decline in palpebral fissure symmetry over time for IFP cases (slope = –0.060, SE = 0.009, $p < 0.001$). The pucker expression, which showed a significant static asymmetry between sides, exhibited the most rapid temporal decline, with the ratio beginning to decrease almost immediately and reaching a minimum of 0.73. This was reflected in the steepest slope (slope = –0.196, SE = 0.011, $p < 0.001$). The smile expression followed an intermediate pattern, with a steady decline over time and a minimum ratio of 0.80. Although smile did not show a statistically significant overall reduction between hemifaces from rest (27.1% vs. 22.5%) or compared with controls (23.2%, $p = 0.09$), the temporal trend revealed progressive asymmetry (slope = –0.109, SE = 0.008, $p < 0.001$) (Fig. 4). This trend was consistent with the significant hemiface difference observed at peak

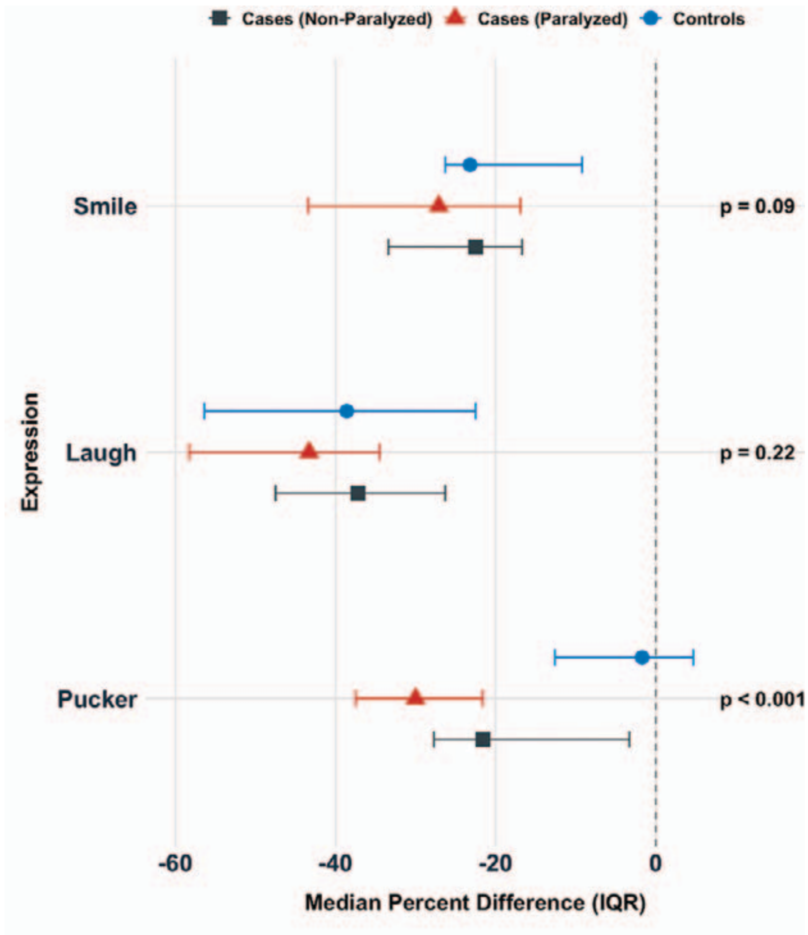

Fig. 3. Percent Change in Palpebral Fissure Dimensions from Rest Across Facial Expressions. Median percent changes (IQR indicated by error bars) in palpebral fissure area from resting state to peak expression during smile, laugh, and pucker expressions for controls, the paralyzed side, and the non-paralyzed side in idiopathic facial paralysis (IFP) patients. The greatest asymmetry occurred during pucker, with the paralyzed side showing a significantly larger reduction than both the non-paralyzed side and controls ($p < 0.001$). No significant group differences were observed during smile or laugh expressions. *P*-values reflect Kruskal-Wallis comparisons across groups for each expression.

smile, where the paralyzed and non-paralyzed palpebral fissures differed by a median of 14.96 mm^2 ($p = 0.018$).

Discussion

This study provides an objective, dynamic evaluation of oral-ocular synkinesis in longstanding IFP using DynaFace, a novel video-based AI tool for automated facial landmark tracking. By quantifying temporal changes in palpebral fissure aperture during elicited oral movements, we identified movement-specific patterns of oral-ocular coordination in patients with IFP compared to healthy controls.

Table 1. Impact of paralysis duration on palpebral fissure changes in IFP patients

Expression	*Duration on paralyzed hemiface*	*p value*	*Duration on Non-Paralyzed hemiface*	*p value*
Smile	–0.014 ± 0.032	0.66	–0.040 ± 0.033	0.24
Laugh	0.032 ± 0.034	0.36	–0.031 ± 0.035	0.39
Pucker	0.005 ± 0.031	0.89	0.007 ± 0.033	0.84

Estimates (±standard error) from univariate linear regression models on palpebral fissure area of both paralyzed and non-paralyzed sides in idiopathic facial paralysis (IFP) patients across smile, laugh, and pucker expressions. Models assess the independent effect of duration on palpebral fissure measurements. No significant estimates were found.

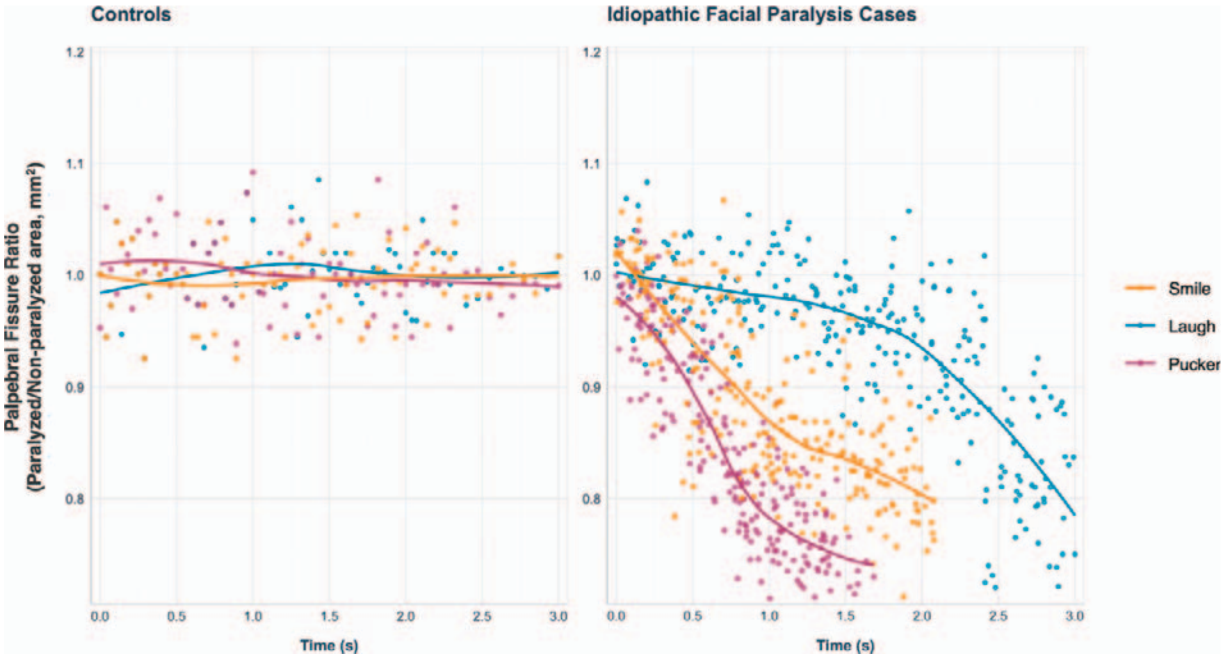

Fig. 4. Temporal Dynamics of Palpebral Fissure Ratios in Controls and Idiopathic Facial Paralysis (IFP) Cases. LOESS (Locally Estimated Scatterplot Smoothing) curves depict the palpebral fissure area ratio (paralyzed to non-paralyzed side) over time during smile, laugh, and pucker expressions. In controls (left panel), ratios remain stable near 1.0, reflecting minimal asymmetry. In contrast, IFP cases (right panel) demonstrate distinct expression-dependent declines in symmetry. Linear regression models were fitted to quantify the rate of change over time. Puckering showed the steepest and most rapid decline (slope = –0.196, SE = 0.011, $p < 0.001$). Smiling showed a moderate decline (slope = –0.109, 95% CI: SE = 0.008, $p < 0.001$), and laughing revealed the most gradual slope (slope = –0.060, SE = 0.009, $p < 0.001$).

In normal individuals, eyelid aperture changes subtly during smiling, laughing, and puckering, reflecting physiological neuromuscular coupling.[29–31] In patients recovering from IFP (≥12 months post-onset), these couplings can become distorted, producing synkinetic orbicularis oculi activation during non-ocular tasks.[3,4] While eyelid aperture was symmetric at rest in both patients and controls, dynamic facial expressions—particularly puckering—revealed marked inter-eye asymmetry in patients with IFP.

In our cohort, asymmetrical eyelid narrowing was detected during all three oral expressions studied, but only puckering produced a statistically significant reduction on the affected side. This stronger association likely reflects coordinated neuromuscular control of the orbicularis oris and orbicularis oculi at the level of the facial motor nucleus. Consistent with this, Ogawara et al. reported that botulinum toxin injection into the orbicularis oculi not only alleviated ocular spasms but also reduced orbicularis oris hyperactivity in patients with hemifacial spasm, supporting the presence of central coupling within the facial nucleus.[32] Because puckering requires sustained, high-intensity activation solely of the orbicularis oris, it likely delivers the strongest drive to this shared circuitry, producing more pronounced involuntary eyelid closure than smiling or laughing.[33,34] Clinically, puckering therefore emerges as a sensitive "stress test" for oral-ocular synkinesis, useful for detecting subtle cases, guiding treatment, and tracking response to interventions such as botulinum toxin, neuromuscular retraining, or selective myectomy and neurolysis. Incorporating it into standardized facial assessments could improve diagnostic accuracy and provide a reliable outcome measure.

A key strength of DynaFace is its ability to track palpebral fissure aperture continuously throughout an expression, capturing the full temporal profile of eyelid movement rather than reducing observations to a single static score. This objective, dynamic measurement quantifies synkinesis as a time-dependent variable, revealing subtle or transient changes that conventional grading often overlooks. In controls, eyelid symmetry (inter-eye ratio ~ 1.0) was stable across expressions. In idiopathic facial paralysis (IFP), however, asymmetries were expression-specific: puckering induced the steepest and most rapid decline in symmetry, smiling produced an intermediate response, and laughing a more delayed yet still cumulative reduction in hemifacial symmetry. These findings suggest that characterizing both the magnitude and timing of asymmetry may allow clinicians to monitor severity, track treatment effects, and tailor therapy over time.

The temporal dimension adds nuance beyond magnitude alone. The rapid onset of asymmetry during puckering suggests strong, immediate co-activation of orbicularis oculi with orbicularis oris, supporting puckering as a sensitive stress test for oral-ocular coupling. By contrast, the delayed asymmetry during laughing likely reflects recruitment of broader muscle groups, producing less immediate but cumulative eyelid narrowing.[35] Clinically, differentiating when synkinesis emerges may refine diagnostics and guide targeted retraining; early-onset puckering asymmetry may warrant focused control of sphincteric muscles, while gradual changes during laughing may require broader coordination training across multiple facial muscle groups.

Interestingly, in this cohort—all with ≥12 months of IFP—the severity of oral-ocular synkinesis did not correlate with duration, suggesting that once established, its manifestation reflects intrinsic neural reorganization rather than progressive exacerbation. While synkinesis is often attributed to misdirected axonal regeneration, our expression-specific findings implicate more proximal changes within the facial motor network. Neurophysiological studies support this multifactorial model: chronic injury may lead to persistent demyelination, remodeling of the Nodes of Ranvier, and altered ion channel distribution, lowering thresholds and predisposing to hyperexcitability.[4,9,36] These changes facilitate ephaptic transmission, or abnormal cross-talk between axons, and strengthen aberrant coupling between the orbicularis oris and orbicularis oculi, consistent with the expression-specific dynamics observed here.[3,4,9] Such central and proximal alterations likely manifest as stable, expression-specific, and non-random patterns of synkinesis, reinforcing the importance of early recognition and intervention before maladaptive circuits become fixed.

This study also introduces DynaFace as a next-generation platform for facial analysis. By integrating deep machine-learning-based landmark detection with high-resolution temporal tracking of 95 landmarks, it provides sub-millimeter precision, reproducible outputs, and individualized movement profiles, offering a level of granularity and reproducibility not achievable with conventional grading systems. Unlike static photographs, DynaFace captures the full sequence of movement, generating time-series data from onset through peak to resolution, reducing the variability inherent in visual grading. The present findings, particularly the expression-specific, time-dependent asymmetries observed during puckering, smiling, and laughing, highlight the nuanced facial dynamics that DynaFace is built to detect, quantify, and track over time. Because outputs are numeric and reproducible, they can objectively monitor changes across visits, for example, reductions in slope or amplitude of eyelid asymmetry after botulinum toxin injection, neuromuscular retraining, or surgery.

The ability to generate expression-specific synkinesis signatures allows clinicians to identify each patient's most vulnerable movement patterns, tailor rehabilitation exercises accordingly, and track progress in specific functional deficits. These strengths align with emerging literature showing that AI-based facial landmark detection achieves high accuracy even in post-paralysis morphologies;[37–40] DynaFace extends this capability into the temporal domain, where synkinesis is best expressed.

By capturing what moves, by how much, and when, DynaFace provides a comprehensive, data-driven portrait of facial function and bridges diagnostic assessment, outcome measurement, and personalized rehabilitation planning within a single platform. As demonstrated here, it not only quantifies the magnitude of oral-ocular synkinesis but also expression-specific onset and rate—parameters critical for patient-specific management. We believe DynaFace represents a next generation of facial analysis, with applications extending beyond facial paralysis into any field requiring precise, objective characterization of facial dynamics.

There are limitations to note: the small sample size and cross-sectional design constrain generalizability and preclude evaluation of how synkinetic patterns evolve over time or in response to treatment. Additionally, while DynaFace was validated against manual review and geometric benchmarks, further studies across larger, more diverse cohorts are needed to confirm robustness in varied clinical contexts. Future longitudinal investigations should track progression, assess demographic influences, and evaluate treatment effects.

Conclusions

This study highlights the value of dynamic, objective analysis for characterizing oral-ocular synkinesis in longstanding IFP. With DynaFace, we identified expression-specific, time-dependent asymmetries in palpebral fissure dynamics, most pronounced during puckering. These findings illuminate the neural coupling between the orbicularis oris and orbicularis oculi and the functional consequences of synkinesis. Beyond providing mechanistic insight, DynaFace emerges as a next-generation platform distinguished by temporal granularity, quantitative precision, and individualized movement profiling. Its ability to reproducibly capture and track synkinetic patterns has direct implications for surgical planning, targeted rehabilitation, treatment monitoring, and patient counseling. Future longitudinal work will determine how these metrics evolve with therapy, enabling more personalized, data-driven management of facial nerve disorders.

Authors' Contributions

Conceptualization: A.R. and K.D.O.B. Methodology: A.R. and K.D.O.B. Investigation: A.R. and K.D.O.B. Visualization: A.R. Formal analysis: A.R. Writing—original draft: A.R. Writing—review and editing: A.R., K.D.O.B., S.C.D., J.N., J.H., and A.D. Software: J.H. Validation: A.D., J.N., S.C.D., and K.D.O.B. Supervision: K.D.O.B.

Author Disclosure Statement

No competing financial interests exist.

Funding Information

None.

Supplementary Material

Supplementary Video

References

1. Marson AG, Salinas R. Bell's palsy. *West J Med.* 2000;173(4):266–268; doi: 10.1136/EWJM.173.4.266
2. Aronowitz P, Harris ES. Facial synkinesis after Bell palsy. *Ann Intern Med Clin Cases.* 2023;2(8); doi: 10.7326/AIMCC.2023.0685
3. Boahene KDO. Etiology, epidemiology, and pathophysiology of post-facial paralysis synkinesis. In: *Management of Post-Facial Paralysis Synkinesis.* Published online January 1, 2021:13–17. doi:10.1016/B978-0-323-67331-0.00002-6
4. Moran CJ, Neely JG. Patterns of facial nerve synkinesis. *Laryngoscope.* 1996;106(12 Pt 1):1491–1496; doi: 10.1097/00005537-199612000-00009
5. Maria CM, Kim J. Individualized management of facial synkinesis based on facial function. *Acta Otolaryngol.* 2017;137(9):1010–1015; doi: 10.1080/00016489.2017.1316871
6. Kleiss IJ, Hohman MH, Quatela OE, et al. Computer-assisted assessment of ocular synkinesis: A comparison of methods. *Laryngoscope.* 2013;123(4):879–883; doi: 10.1002/LARY.23778
7. Husseman J, Mehta RP. Management of synkinesis. *Facial Plast Surg.* 2008;24(2):242–249; doi: 10.1055/S-2008-1075840
8. Baker RS, Stava MW, Nelson KR, et al. Aberrant reinnervation of facial musculature in a subhuman primate: A correlative analysis of eyelid kinematics, muscle synkinesis, and motoneuron localization. *Neurology.* 1994;44(11):2165–2173; doi: 10.1212/WNL.44.11.2165
9. Crumley RL. Mechanisms of synkinesis. *Laryngoscope.* 1979;89(11):1847–1854; doi: 10.1288/00005537-197911000-00020
10. Thomander L. Reorganization of the facial motor nucleus after peripheral nerve regeneration: An HRP study in the rat. *Acta Otolaryngol*. 1984;97(5–6):619–626; doi: 10.3109/00016488409132939
11. Nacimiento W, Podoll K, Graeber MB, et al. Contralateral early blink reflex in patients with facial nerve palsy: Indication for synaptic reorganization in the facial nucleus during regeneration. *J Neurol Sci.* 1992;109(2):148–155.
12. Choi D, Raisman G. Somatotopic organization of the facial nucleus is disrupted after lesioning and regeneration of the facial nerve: The histological representation of synkinesis. *Neurosurgery*. 2002;50(2):355–362; doi: 10.1097/00006123-200202000-00022
13. Shokri T, Patel S, Ziai K, et al. Facial synkinesis: A distressing sequela of facial palsy. *Ear Nose Throat J.* 2024;103(6):NP382–NP391; doi: 10.1177/01455613211054627
14. Mabvuure NT, Hallam MJ, Venables V, et al. Validation of a new photogrammetric technique to monitor the treatment effect of botulinum toxin in synkinesis. *Eye (Lond)*. 2013;27(7):860–864; doi: 10.1038/eye.2013.91
15. van Veen MM, Dusseldorp JR, Hadlock TA. Long-term outcome of selective neurectomy for refractory periocular synkinesis. *Laryngoscope.* 2018;128(10):2291–2295; doi: 10.1002/LARY.27225
16. Isono M, Murata K, Tanaka H, et al. An objective evaluation method for facial mimic motion. *Otolaryngol Head Neck Surg.* 1996;114(1):27–31; doi: 10.1016/S0194-59989670279-6
17. Rogers CR, Schmidt KL, Vanswearingen JM, et al. Automated facial image analysis: Detecting improvement in abnormal facial movement after treatment with botulinum toxin A. *Ann Plast Surg.* 2007;58(1):39–47; doi: 10.1097/01.SAP.0000250761.26824.4F
18. Wu ZB, Silverman CA, Linstrom CJ, et al. Objective computerized versus subjective analysis of facial synkinesis. *Laryngoscope.* 2005;115(12):2118–2122; doi: 10.1097/01.MLG.0000182811.49686.76
19. Linstrom CJ. Objective facial motion analysis in patients with facial nerve dysfunction. *Laryngoscope.* 2002;112(7 Pt 1):1129–1147; doi: 10.1097/00005537-200207000-00001
20. Mehta RP, Wernickrobinson M, Hadlock TA. Validation of the synkinesis assessment questionnaire. *Laryngoscope.* 2007;117(5):923–926; doi: 10.1097/MLG.0B013E3180412460
21. Coulson SE, Croxson GR, Adams RD, et al. Reliability of the "Sydney," "Sunnybrook," and "House Brackmann" facial grading systems to assess voluntary movement and synkinesis after facial nerve paralysis. *Otolaryngol Head Neck Surg.* 2005;132(4):543–549; doi: 10.1016/j.otohns.2005.01.027
22. House JW, Brackmann DE. Facial nerve grading system. *Otolaryngol Head Neck Surg*. 1985;93(2):146–147; doi: 10.1177/019459988509300202
23. Vrabec JT, Backous DD, Djalilian HR, et al.; Facial Nerve Disorders Committee. Facial nerve grading system 2.0. *Otolaryngol Head Neck Surg.* 2009;140(4):445–450; doi: 10.1016/J.OTOHNS.2008.12.031
24. Ross BG, Fradet G, Nedzelski JM. Development of a sensitive clinical facial grading system. *Otolaryngol Head Neck Surg.* 1996;114(3):380–386; doi: 10.1016/S0194-59989670206-1
25. Hartley H, Blumenow W, Williams R, et al. Assessment and grading of synkinesis and facial palsy. *In: Management of Post-Facial Paralysis Synkinesis*. 2022:51–58; doi: 10.1016/B978-0-323-67331-0.00007-5 Published online January 1
26. Schroff F, Kalenichenko D, Philbin J. FaceNet: A unified embedding for face recognition and clustering. *2015 IEEE Conference on Computer Vision and Pattern Recognition (CVPR)*, Boston, MA, USA, Published online 2015:815–823.
27. Prados-Torreblanca A, Buenaposada JM, Baumela L. Shape preserving facial landmarks with graph attention networks. In: *BMVC 2022–33rd British Machine Vision Conference Proceedings*. Published online October 13, 2022. https://arxiv.org/pdf/2210.07233 Accessed August 4, 2025.
28. Kimura T, Narita K, Oyamada K, et al. Fine-tuning on AI-driven video analysis through machine learning: Development of an automated evaluation tool of facial palsy. *Plast Reconstr Surg.* 2025;155(6):1071e–1081e; doi: 10.1097/PRS.0000000000011924
29. Feng G, Zhuang Y, Gao Z. Measurement and analysis of associated mimic muscle movements. *J Otol.* 2015;10(1):39–45; doi: 10.1016/J.JOTO.2015.06.001
30. Root AA, Stephens JA. Organization of the central control of muscles of facial expression in man. *J Physiol.* 2003;549(Pt 1):289–298; doi: 10.1113/JPHYSIOL.2002.035691
31. Dibeklioğlu H, Salah AA, Gevers T. Are you really smiling at me? Spontaneous versus posed enjoyment smiles. *In: Lecture Notes in Computer Science*. 2012;7574 LNCS(PART 3):525–538; doi: 10.1007/978-3-642-33712-3_38
32. Ogawara K, Kuwabara S, Kamitsukasa I, et al. Trigeminal afferent input alters the excitability of facial motoneurons in hemifacial spasm. *Neurology.* 2004;62(10):1749–1752; doi: 10.1212/01.WNL.0000125183.81555.E4
33. Rocha DD, Barboza CR, Furlan RMMM, et al. Analysis of different tasks to normalize the electrical signal of the orbicularis oris muscle by maximum voluntary contraction: Pilot study. *Audiol Commun Res*. 2021;26:e2400; doi: 10.1590/2317-6431-2020-2400
34. Schumann NP, Bongers K, Scholle HC, et al. Atlas of voluntary facial muscle activation: Visualization of surface electromyographic activities of facial muscles during mimic exercises. *PLoS One*. 2021;16(7):e0254932; doi: 10.1371/journal.pone.0254932
35. Tanaka M, Sumitsuji N. Electromyographic study of facial expressions during pathological laughing and crying. *Electromyogr Clin Neurophysiol.* 1991;31(7):399–406. Accessed August 16, 2025.
36. Sadjadpour K. Postfacial palsy phenomena: Faulty nerve regeneration or ephaptic transmission? *Brain Res*. 1975;95(2–3):403–406; doi: 10.1016/0006-8993(75)90117-1

37. Almarhoumi AA. Accuracy of artificial intelligence in predicting facial changes post-orthognathic surgery: A comprehensive scoping review. *J Clin Exp Dent.* 2024;16(5):e624–e633; doi: 10.4317/JCED.61500
38. Gaber A, Taher MF, Wahed MA, et al. Classification of facial paralysis based on machine learning techniques. *Biomed Eng Online.* 2022;21(1):65–20; doi: 10.1186/S12938-022-01036-0
39. Shi H, Fan Y, Zhang Y, et al. Intelligent Bell facial paralysis assessment: A facial recognition model using improved SSD network. *Sci Rep.* 2024;14(1):1–11; doi: 10.1038/s41598-024-63478-x
40. Park I, Park JH, Yoon J, et al. Machine learning model of facial expression outperforms models using analgesia nociception index and vital signs to predict postoperative pain intensity: A pilot study. *Korean J Anesthesiol.* 2024;77(2):195–204; doi: 10.4097/KJA.23583